

## Numerical comparison of the seismic performance of steel rings in off-centre bracing system and diagonal bracing system

Mohammad Bazzaz<sup>\*</sup>, Zahra Andalib<sup>a</sup>, Ali Kheyroddin<sup>b</sup> and Mohammad Ali Kafi<sup>c</sup>

*Faculty of Civil Engineering, Semnan University, Semnan, Iran*

*(Received April 24, 2014, Revised September 08, 2014, Accepted March 20, 2015)*

**Abstract.** During a seismic event, a considerable amount of energy is input into a structure. The law of energy conservation imposes the restriction that energy must either be absorbed or dissipated by the structure. Recent earthquakes have shown that the use of concentric bracing system with their low ductility and low energy dissipation capacity, causes permanent damage to structures during intense earthquakes. Hence, engineers are looking at bracing system with higher ductility, such as chevron and eccentric braces. However, braced frame would not be easily repaired if serious damage has occurred during a strong earthquake. In order to solve this problem, a new bracing system an off-centre bracing system with higher ductility and higher energy dissipation capacity, is considered. In this paper, some numerical studies have been performed using ANSYS software on a frame with off-centre bracing system with optimum eccentricity and circular element created, called OBS\_C\_O model. In addition, other steel frame with diagonal bracing system and the same circular element is created, called DBS\_C model. Furthermore, linear and nonlinear behavior of these steel frames are compared in order to introduce a new way of optimum performance for these dissipating elements. The obtained results revealed that using a ductile element or circular dissipater for increasing the ductility of off-centre bracing system and centric bracing system is useful. Finally, higher ductility and more energy dissipation led to more appropriate behavior in the OBS\_C\_O model compared to DBS\_C model.

**Keywords:** finite elements; numerical analysis; braced frame; damping; building; knee brace; steel structure

---

### 1. Introduction

Extensive research has been conducted to increase the ductility of concentric braces over the past two decades. Despite some benefits such as ease of implementation and reconstruction, their low ultimate displacement has created concerns about their application. Moreover, limited ductility

---

\*Corresponding author, M.Sc., E-mail: [M\\_Bazzaz@sun.semnan.ac.ir](mailto:M_Bazzaz@sun.semnan.ac.ir)

<sup>a</sup> M.Sc., E-mail: [Z\\_Andalib@sun.semnan.ac.ir](mailto:Z_Andalib@sun.semnan.ac.ir)

<sup>b</sup> Professor, Ph.D., E-mail: [kheyroddin@semnan.ac.ir](mailto:kheyroddin@semnan.ac.ir)

<sup>c</sup> Assistant Professor, Ph.D., E-mail: [mkafi@semnan.ac.ir](mailto:mkafi@semnan.ac.ir)

of concentric braces has caused poor functionality against earthquake (Lotfollahi and Mofid 2008, Hsu *et al.* 2011). Furthermore, valuable studies, such as using a circular element with hyper elastic material in a toggle bracing frame (Murthy 2005), has been conducted in order to increase the ductility. Most of these methods, however, are either confined to specific types of braces or need special materials or customized technology. Utilizing energy absorbers such as a steel ring and a controlling fuse have been proposed in order to solve these problems (Marshall *et al.* 2010a, b). The off-centre bracing system with high ductility and energy dissipation capacity of large earthquakes was used (Moghaddam and Estekanchi 1995, Amadio *et al.* 2008, Annan *et al.* 2009).

The present paper aims to investigate the behavior of a steel ring as a ductile element installed at the end of various braced members. The utilization of steel ring as proposed in this paper is a completely new idea that is under investigation for the first time (Bazzaz *et al.* 2012). However, the optimum behavior of steel ring has been proved in other papers (Bazzaz *et al.* 2014, Abbasnia *et al.* 2008). In addition, the frames with steel ring have more ductility and energy dissipation capacity compared to eccentric braces without steel ring. Finally, numerical observations (Bazzaz *et al.* 2012, 2015) show that the structural members of the bracing system remain in their elastic zone, except the steel ring. Moreover, the destruction is limited to the steel ring.

## 2. Literature review: Recent studies

The classical energy conversation law is described in the following form for structural engineering applications.

$$E_i = E_k + E_s + E_h + E_d \quad (1)$$

Where Eq. (1)  $E_i$  is energy input into the system from the earthquake,  $E_k$  is the kinetic energy,  $E_s$  is the recoverable strain energy,  $E_h$  is the irrecoverable energy due to dissipation from the inherent damping and  $E_d$  is dissipated energy due to supplemental devices. Passive energy dissipation systems, unlike active energy dissipation systems, do not require external power to generate system control forces. Hence, they are easier and cheaper to implement in a structure (Murthy 2005).

In the previous studies an off-centre bracing system was introduced (Moghaddam and Estekanchi 1995, 1999). As shown in Fig. 1, an off-centre bracing system basically consists of the non straight tension strut BOC with an eccentricity designated as  $e$ . The midpoint  $O$  is connected to the corner by the third member  $AO$ . Once the load is applied, all these three members are stretched, therefore, act in tension. As the load increases, the original geometry changes and a new formulation of equilibrium equations based on the new geometry is required. Therefore, the characteristics of such an off-centre system are geometrically nonlinear. An earlier investigation (Moghaddam and Estekanchi 1999) revealed that the degree of nonlinearity depends mainly on the amount of eccentricity and the relative stiffness of the third bracing member. It was also shown that this nonlinear behavior could be employed for mitigation of seismic loads. In the former study all the models were assumed to be elastic.

Genetic algorithms on the optimal size and location of dampers have been presented (Singh and Moreschi 2002). Also, other comprehensive investigations on the buckling and damping in Y-braced and X-braced frame have been suggested for managing seismic loads (Majidzamani and Rasouli 2006, Majidzamani *et al.* 2011).

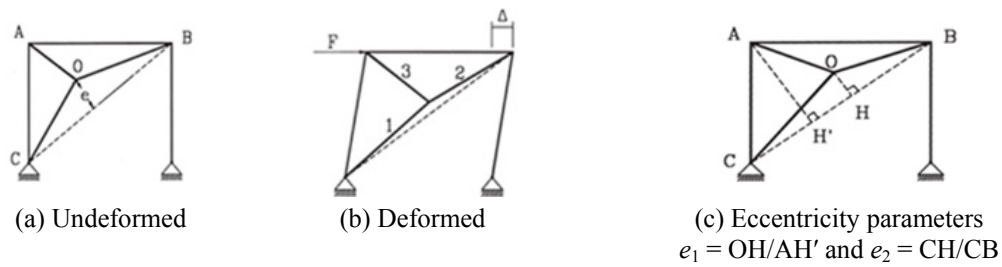


Fig. 1 Off-centre bracing system. (Andalib *et al.* 2010)

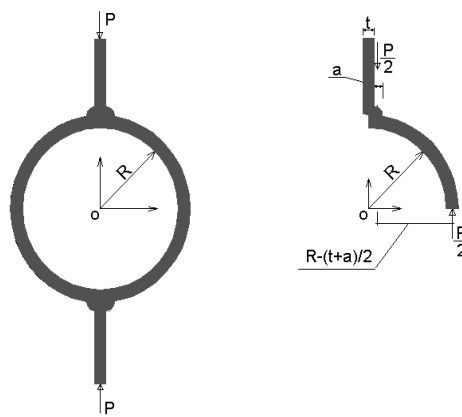


Fig. 2 Schematic of the ring

The researchers worked on the optimum placement of bracing members and introduced 31° as an optimum degree (Murthy 2005). Using ring as an energy dissipation has not been considered. In addition, steel ring was introduced as a capable energy dissipater in another study and diagonal braced frame with circular element was experimented (Abbasnia *et al.* 2008). High ductility, high energy dissipation and decrease in base shear were the valuable achievements of this study.

### 3. Geometrical specification of models

#### 3.1 Geometrical specification of the ring

The material strength relationships between force and variation of the ring diameter and its internal forces in the elastic zone under load  $P$  are shown in Fig. 2 and the following equations from Eqs. (2)-(8) (Roark 1990).

$$M^+ = 0.3183PR \quad \theta = \frac{\pi}{2} \quad (2)$$

$$M^- = 0.1817PR \quad \theta = 0 \quad (3)$$

$$I = \frac{1}{12}t^3l \quad (4)$$

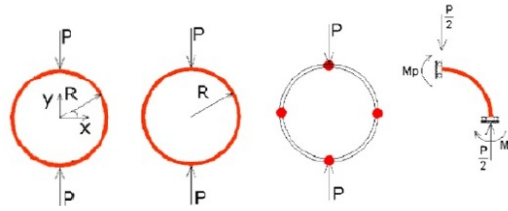


Fig. 3 Plastic hinge formation

$$\delta_y = -0.149 \frac{PR^3}{EI} \quad (5)$$

$$\delta_x = +0.137 \frac{PR^3}{EI} \quad (6)$$

$$T = \frac{1}{2} P \cos \theta \quad (7)$$

$$V = -\frac{1}{2} P \sin \theta \quad (8)$$

By increasing the load, four plastic hinges are produced in the ring, as shown in Fig. 3, and the balance relationship in the plastic limit state are as following equations from Eqs. (9) to (11)

$$2M_p = \frac{PR}{2} \Rightarrow P = \frac{4M_p}{R} \quad (9)$$

$$M_p = \frac{t^2 l \sigma_y}{4} \quad (10)$$

$$P = \frac{t^2 l \sigma_y}{R} \quad (11)$$

As observed, the bearing load capacity of the ring is directly correlated with its length, yielding stress, and ring thickness squared and it is inversely correlated with its radius. According to achieved bearing capacity of steel ring, a ring is considered with external diameter of 220 mm and thickness of 12 mm.

### 3.2 Geometrical specification of frame with diagonal brace and ductile element

For analytical results, a hinged frame with diagonal bracing and steel ring at the end in a single-bay single-story frame was created which is called DBS-C model for simplification. Additionally, the purpose of embedding steel ring at the end of brace member is to increase ductility of brace considering buckling control. Hence, it is necessary for bearing capacity of steel ring at end of brace member to be less than buckling load of brace. Therefore, it is necessary to determine buckling load of brace before designing steel ring dimensions, as shown in Fig. 4.

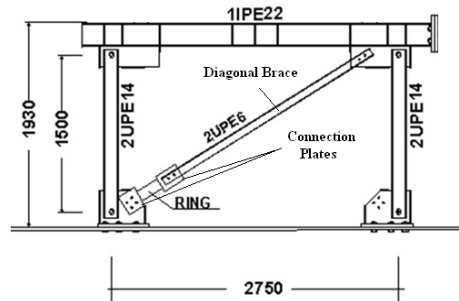


Fig. 4 Hinged frame with bracing diagonal and steel ring model (DBS-C model)

Table 1 Specification of the frame sections with diagonal bracing and the steel ring (DBS-C model)

Specification	Brace	Beam	Column	Members
	Kind of profile	2UNP14	IPE22	2UNP6
Common in Model DBS-C	$A$ (mm <sup>2</sup> )	4080	3950	1292
	$I_x$ (mm <sup>4</sup> )	12100000	30600000	632000
	$I_y$ (mm <sup>4</sup> )	4339500	1620000	561500
	$r_x$ (mm)	54.5	88	22.1
	$r_y$ (mm)	32.6	20.2	20.8
	$l$ (mm)	1500	2750	2860

Designing the frame sections except steel ring is based on elastic behavior and low axial displacement. Hence, connections modeled as pin assuming pin connections are more conservative, specification of frame is shown in Table 1.

The present paper does not deal with the determination of safety factor between the buckling load of brace and bearing capacity of steel ring. On the other hand, it is necessary to determine steel ring capacity for designing a steel ring. In order to achieve this goal, damaging safety factor of steel ring before buckling of brace of 1.5 is assumed. Ultimately steel ring with 112.16 kN bearing capacity is suitable to be embedded at the end of diagonal bracing.

According to achieved bearing capacity of steel ring, a ring is considered taking external diameter of 220 mm, thickness 12 mm and a length of 140 mm.

### 3.3 Geometrical specifications of frame with off-centre braced frame and ductile element in the optimum place

The goal of embedding circular element in the concentric bracing system is to increase ductility with buckling control. However, the bearing capacity of circular element is limited. Hence, the frame ductility would be decreased with increasing the ring diameter. Moreover, considering the architectural limitation, circular element is used in an off-centre bracing system as shown in Fig. 4. Using this system result in exerting lower force to ductile element and tolerated greater force with suitable ductility.

Bearing capacity of ductile element embedded at the end of bracing members should be less than buckling force of braces. Hence, before designing dimensions of a circular element,

Table 2 Sections specification of the hinged frame with off-centre bracing system and the ductile element

Specification	Brace	Column	Beam	Brace OA	Brace OB	Brace OC
	Kind of profile	2UNP14	IPE22	2UNP12	2UNP12	2UNP12
Common in Model OBS-C-O	$A$ (mm <sup>2</sup> )	4080	3950	3400	3400	3400
	$I_x$ (mm <sup>4</sup> )	12100000	30600000	7280000	7280000	7280000
	$I_y$ (mm <sup>4</sup> )	4339500	1620000	3162400	3162400	3162400
	$r_x$ (mm)	54.5	88	46.27	46.27	46.27
	$r_y$ (mm)	32.6	20.2	30.5	30.5	30.5
	$l$ (mm)	1500	2750	330	2000	1060

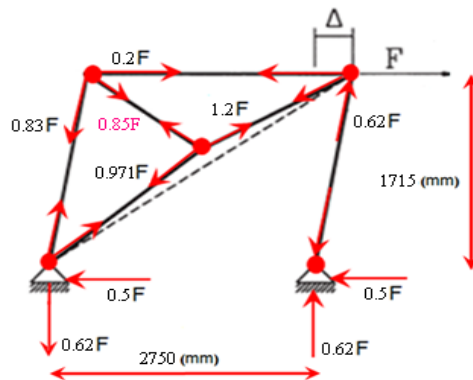


Fig. 5 Preliminary configuration of bracing connection

determination of buckling forces of bracing members is necessary. The sections of profiles are two channels with 20 mm distance from each other. The space between column filler and brace member is 380 mm and the thickness of fillers and plates of corner connection are 20 mm. The specification of frame is shown in Table 2. Moreover, the design of frame sections except circular element is based on elastic behavior and low strain. As shown in Fig. 5, connections modeled as pin, assuming pin joint is more conservative.

The goal of investigating these models is to reach optimum use of circular element (Andalib *et al.* 2010, 2014, Bazzaz *et al.* 2011). Hence, bearing capacity of steel ring with correct safety factor should be less than buckling load. Therefore Circular element is modeled by taking outside diameter 220 mm, thickness 12 mm and a length of 200 mm. In order to design steel elements, AISC-ASD 2005 (American Institute of Steel Construction 2005) code is used. ATC-24 (Applied Technology Council 1996) and FEMA-356 (Federal Emergency Management Agency 2000) codes were used to calculate seismic load.

#### 4. The method of model analysis

Nonlinear static analysis is used in order to investigate the hysteresis behavior of models. The displacement - control criterion is induced for loading of models. The goal of embedding ductile

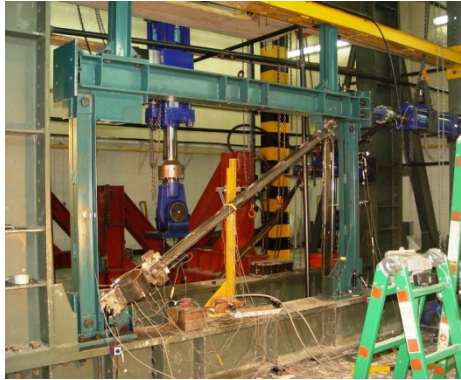


Fig. 6 Diagonal hinged brace frame with ductile element in Laboratory (Abbasnia *et al.* 2008)

element at the end of bracing member is to increase ductility considering buckling control. To achieve this purpose, it is necessary for bearing capacity of ductile element at the end of brace member to be less than buckling force of braces. This fact was considered in the experimental investigation (Abbasnia *et al.* 2008). Therefore, the bearing capacity of this element was considered half of the buckling force of diagonal braced members. Considering the above-mentioned conditions, buckling load is determined before designing dimensions of ductile element. Finally, capacity design method is used to determine the bearing capacity of ductile element, inducing forces to ductile element need to be less than  $0.85 F$ . In other words, the design of the other members is based on the fact that they would be stable before general failure of ductile element.

Therefore, the selected ductile element reaches to collapse inelastic zone, much earlier than buckling of bracing members. Basically, there is no buckling in this system, this item consists of all types of buckling such as inelastic buckling, buckling load and post buckling stiffness. In addition, buckling is controlled in the experimental research (Abbasnia *et al.* 2008). In this research, the ductile element is embedded in the diagonal bracing as shown in Fig. 6. Ductile element can be replaced by another one after failure, without occurring any buckling in the other bracing members.

Concerning all above-mentioned reasons, the Eigen Buckling analysis is conducted at the end of numerical analysis to investigate the brace member buckling and also to prove the accuracy of modeling.

## 5. Validation of numerical analysis with experimental data

To validate analytical results, steel ring is considered as a ductile element which is called (CT20\_TH12\_C) for simplification. Regarding to modeling in the International Institute Earthquake Engineering and Seismology (Abbasnia *et al.* 2008) another ring with external diameter 220 mm, thickness 12 mm and a length of 100 mm with two connections plate  $200 \times 170 \times 12$  mm with 7 mm fillet weld is taken, as shown in Fig. 7.

As shown in Fig. 8, the achieved hysteresis plots of experimental and analytical data have shown very good superposition.

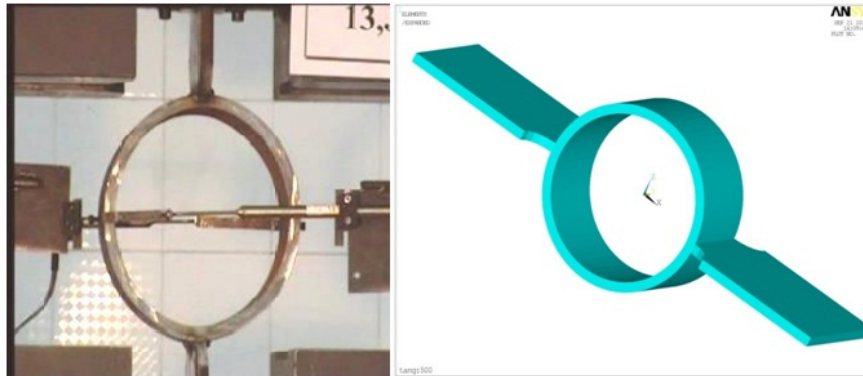


Fig. 7 General view of steel ring in universal jack and ANSYS software

### 6. Monotonic load

Capacity and corresponding drift are important parameters to be compared between monotonic and cyclic tests. Capacity is the most interesting comparison for the designer since current design is based on values obtained from monotonic tests of steel rings.

For years, monotonic loading was the standard method for testing steel materials because it provided a good indication of the performance under one-directional loading and wind loading. Comparing the results of the monotonic tests to the cyclic tests steel rings tend to fatigue and fail at a faster rate than during monotonic loading due to the numerous fully reversed cycles of cyclic loading. Therefore, the need to quantify the reduction is important. Considering 1930 mm height, for modeling frames, according to Eq. (12) a 60 mm storey drift were induced at the top of beam flange.

$$0.03H = 0.03 \times 1930 = 57.9 \text{ mm} \approx 60 \text{ mm} \tag{12}$$

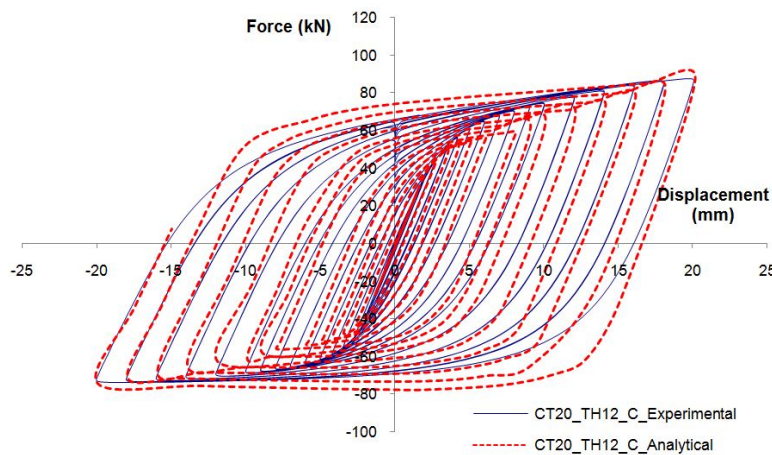


Fig. 8 Comparative hysteresis plots of experimental and analytical results for CT20\_TH12\_C

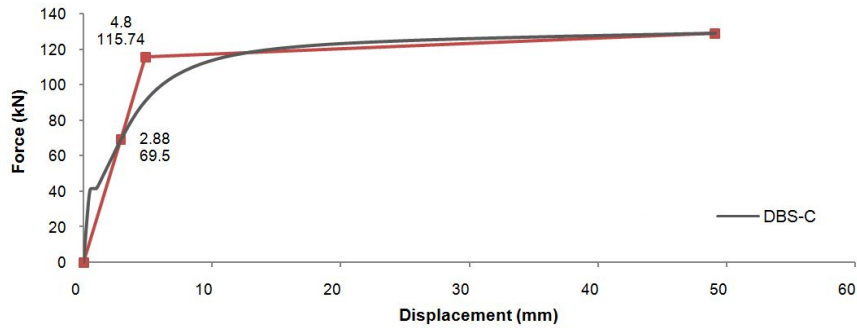


Fig. 9 Bilinear force-displacement curve of DBS-C model

Table 3 Behavioral parameters

Models	$Q_y$ (kN)	$\Delta_y$ (mm)	$K_e$ (kN)	$K'$ (kN)	$Q_{y,0.03}$ (kN)	$E_{Monotonic}$ (J)	$\mu$
Model OBS-C-O	150	6.7	44.64	0.495	196.19	16821	14.93
Model DBS-C	115.74	4.8	24.08	0.303	129.18	5777	10.23

### 6.1 Diagonal braced frame and ductile element

For analytical results, a hinged frame with diagonal bracing and steel ring at the end in a single-bay single-story frame is created which is called DBS-C model for simplification. The purpose of embedding steel ring at the end of brace member is to increase ductility of brace considering buckling control. As shown in Fig. 4, designing frame sections except steel ring is based on elastic behavior and low axial displacement. Connections modeled as pin assuming pin connections are more conservative. Specification of the frame is shown in Table 1. Bilinear force-displacement curve is drawn in Fig. 9, in order to investigate the stiffness, force and yielding displacement of the frame according to FEMA356 (Federal Emergency Management Agency 2000) suggested method. The obtained result is shown in Table 3.

The maximum displacement is 50 mm and the displacement of the system at the end of elastic limit is 4.8 mm. The ductility factor ( $\mu$ ) of this system is

$$\mu = \frac{\Delta_{max}}{\Delta_y} = \frac{50}{4.8} = 10.42 \tag{13}$$

Fig. 10 shows Von Misses stress distribution and Von Misses strain distribution of hinged frame with diagonal bracing system and ductile element.

### 6.2 Off-centre bracing system with ductile element in optimum place

A hinged frame with off-centre bracing and steel ring in optimum place calculated in another paper by (Bazzaz *et al.* 2014), in a single-bay single-story frame is created and it is called OBS-C-O model for simplification. The purpose of embedding steel ring at the end of brace member is to increase ductility of brace considering buckling control. Connections modeled as pin assuming pin connections are more conservative. Specification of the frame is shown in Table 2.

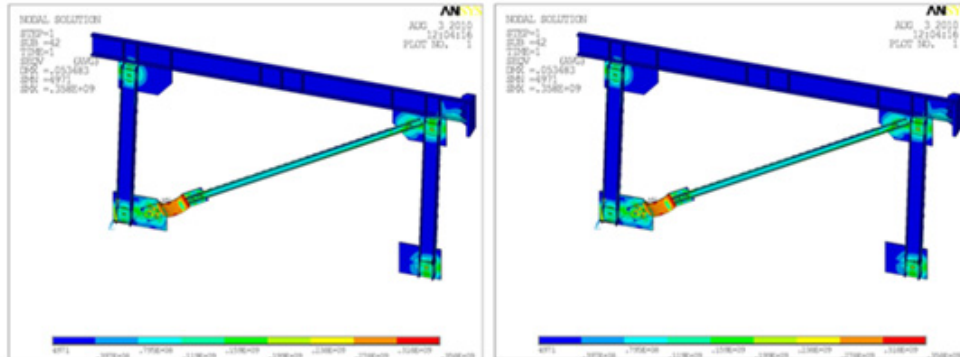


Fig. 10 Von Mises strain and stress under monotonic load for DBS-C Model

Bilinear force-displacement curve is drawn in Fig. 11, in order to investigate the stiffness, force and yielding displacement of the frame according to FEMA356 (Federal Emergency Management Agency 2000) suggested method. The obtained result is shown in Table 3.

The maximum displacement is 100 mm and the displacement of the system at the end of elastic limit is 6.7 mm. The ductility factor ( $\mu$ ) of this system is

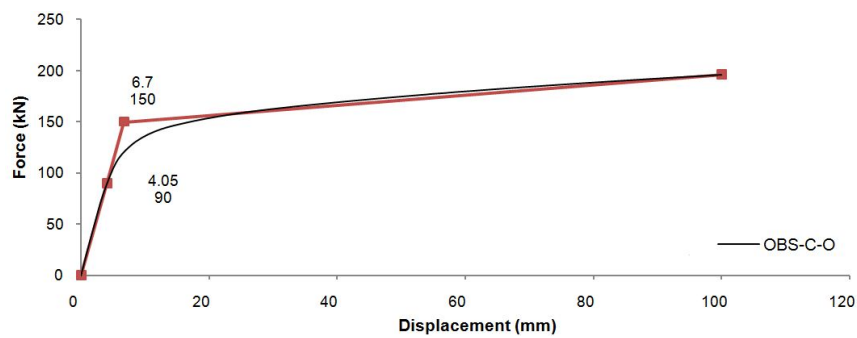


Fig. 11 Bilinear force-displacement curve of OBS-C-O model

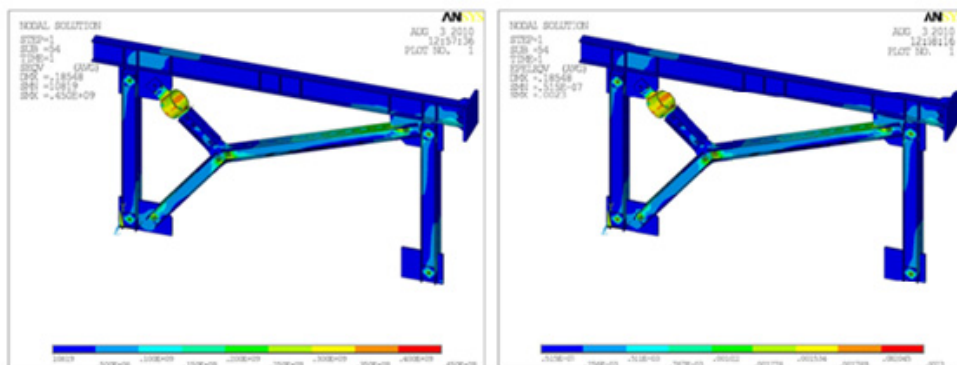


Fig. 12 Von Mises strain and stress under monotonic load for Model OBS-C-O

$$\mu = \frac{\Delta_{\max}}{\Delta_y} = \frac{100}{6.7} = 14.93 \tag{14}$$

Fig. 12 shows Von Misses stress distribution and Von Misses strain distribution of hinged frame with off-centre bracing system and ductile element in the optimum place.

### 7. Cyclic load

The load is reciprocal to simulate earthquake loads. The method of loading is according to the proposed method of ATC\_24 code (Applied Technology Council 1996). In Fig. 13, the loading history of the ATC\_24 code (Applied Technology Council 1996) is shown. Considering ATC\_24 code (Applied Technology Council 1996), the loading history of the models is shown in Table 4.

#### 7.1 Diagonal braced frame and ductile element

The obtained results from the cyclic load analysis of the model as force-displacement plot are presented in Fig. 14. This curve continued to ultimate yielding strain of applied steels. To investigate inelastic behavior, the Von Misses yield surface is used. In this analysis, tolerable tensile load in the nonlinear limit zone is 104.84 kN and tolerable compressive load in the nonlinear limit zone is 109.4 kN. The maximum displacement in the nonlinear zone of 16.1 mm is achieved.

The obtained hysteresis loops are wide and revealed suitable absorption of input energy to the structure. As shown in Fig. 15, the hysteresis loop push force-displacement plot for the frame is

Table 4 Loading history of models in this paper

Cycles	Displacement (mm)		Cycles	Displacement (mm)		Cycles	Displacement (mm)	
Cycle 1	0.115	-0.115	Cycle 16	4.6	-4.6	Cycle 31	11.5	-11.5
Cycle 2	0.1725	-0.1725	Cycle 17	5.06	-5.06	Cycle 32	11.96	-11.96
Cycle 3	0.23	-0.23	Cycle 18	5.52	-5.52	Cycle 33	12.42	-12.42
Cycle 4	0.46	-0.46	Cycle 19	5.98	-5.98	Cycle 34	12.88	-12.88
Cycle 5	0.69	-0.69	Cycle 20	6.44	-6.44	Cycle 35	13.34	-13.34
Cycle 6	0.92	-0.92	Cycle 21	6.9	-6.9	Cycle 36	13.8	-13.8
Cycle 7	1.15	-1.15	Cycle 22	7.36	-7.36	Cycle 37	14.26	-14.26
Cycle 8	1.38	-1.38	Cycle 23	7.82	-7.82	Cycle 38	14.72	-14.72
Cycle 9	1.61	-1.61	Cycle 24	8.28	-8.28	Cycle 39	15.18	-15.18
Cycle 10	1.84	-1.84	Cycle 25	8.74	-8.74	Cycle 40	15.64	-15.64
Cycle 11	2.3	-2.3	Cycle 26	9.2	-9.2	Cycle 41	16.1	-16.1
Cycle 12	2.76	-2.76	Cycle 27	9.66	-9.66	Cycle 42	16.56	-16.56
Cycle 13	3.22	-3.22	Cycle 28	10.12	-10.12	Cycle 43	17.02	-17.02
Cycle 14	3.68	-3.68	Cycle 29	10.58	-10.58	Cycle 44	17.48	-17.48
Cycle 15	4.14	-4.14	Cycle 30	11.04	-11.04	Cycle 45	17.94	-17.94

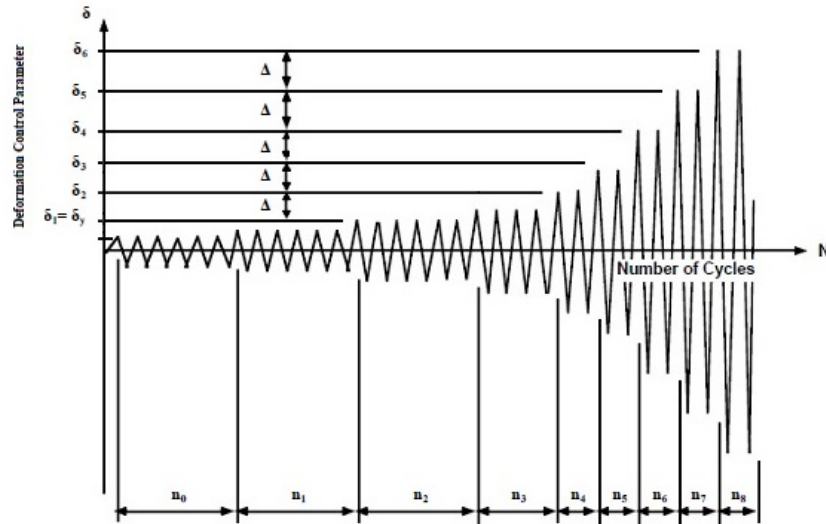


Fig. 13 Loading history in ATC\_24 code (Applied Technology Council 1996)

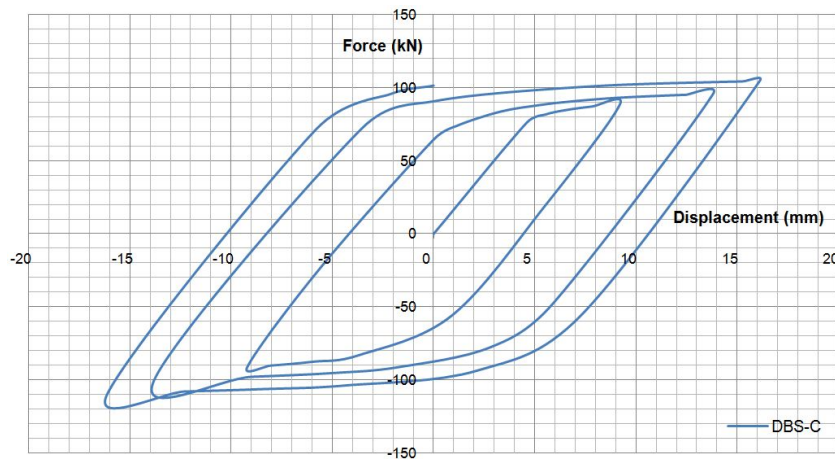


Fig. 14 Force-lateral displacement plot for DBS-C Model

obtained. The maximum tolerable tension load in this system is 104.84 kN maximum displacement is 16.1 mm and the displacement of the system at the end of elastic limit is 4.6 mm. The ductility factor ( $\mu$ ) of this system for tension load is

$$\mu = \frac{\Delta_{max}}{\Delta_y} = \frac{16.1}{4.6} = 3.5 \tag{15}$$

Fig. 16 shows Von Mises stress distribution and Von Mises strain distribution of hinged frame with diagonal bracing system and ductile element. To specify analytical results, the obtained results of studying the loading cycles are shown in Table 5.

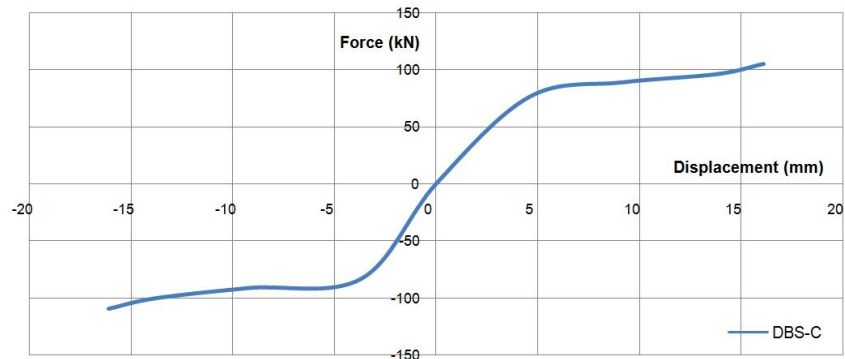


Fig. 15 Hysteresis loop push force-displacement plot for DBS-C Model

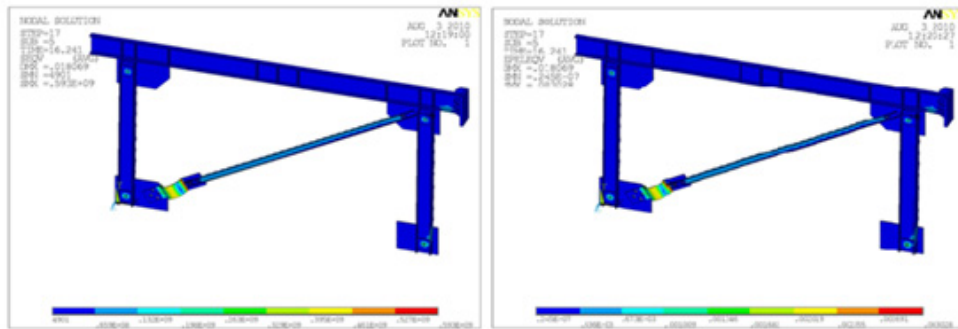


Fig. 16 Von Mises strain and stress under cyclic load for DBS-C Model

Table 5 Analytical results models

Models	$E_{P-max}$ (J)	$E_{E-max}$ (J)	$P_{P-max}$ (kN)	$P_{E-max}$ (kN)	$\frac{E_{P-max}}{E_{E-max}}$	$\frac{P_{P-max}}{P_{E-max}}$	$\left(\frac{E_P}{E_E}\right)_{max}$	$\left(\frac{P_P}{P_E}\right)_{max}$
Model OBS-C-O	23616.14	96.08	219.03	105.57	245.8	2.08	118.17	
Model DBS-C	3916	100	104.84	46.23	39.16	2.27	17.25	

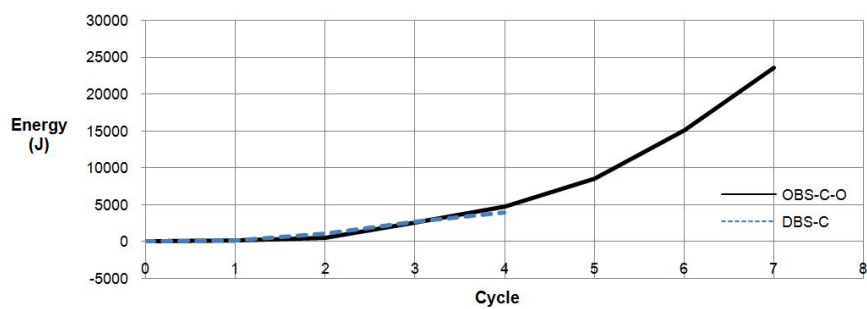


Fig. 17 Comparative energy-loading cycle plots for OBS-C-O and DBS-C models

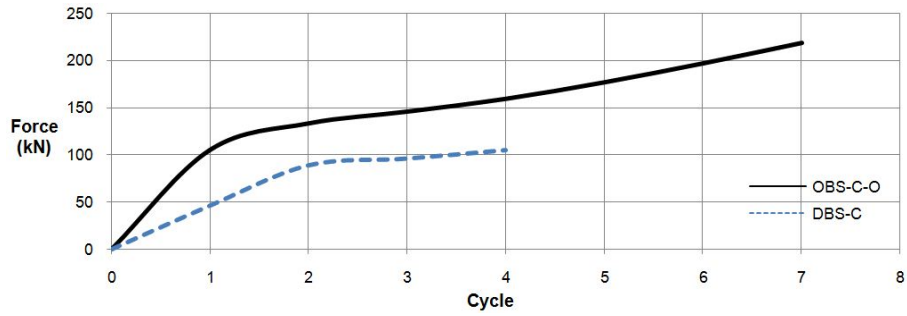


Fig. 18 Comparative force-loading cycle plots for OBS-C-O and DBS-C models

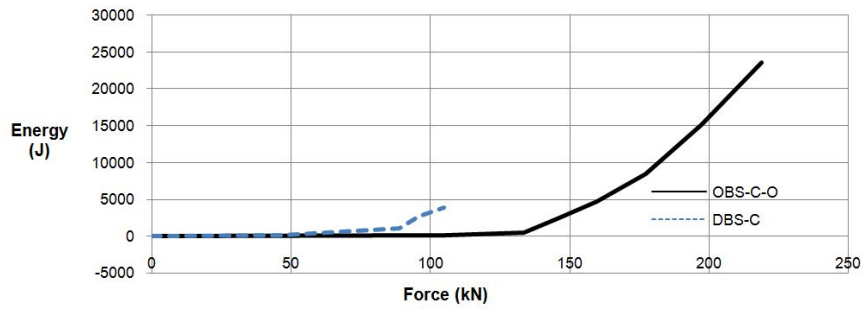


Fig. 19 Comparative force-energy plots for OBS-C-O and DBS-C models

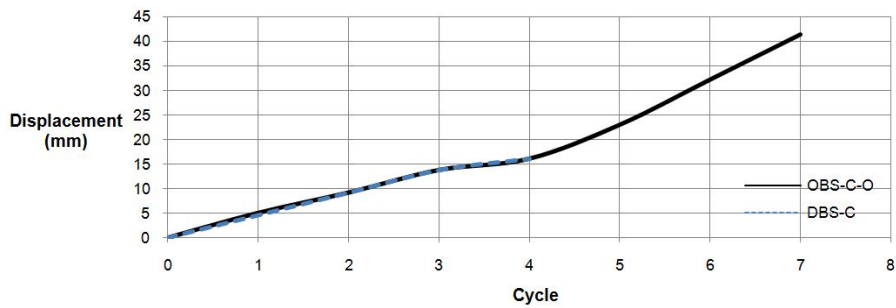


Fig. 20 Comparative lateral displacement-loading cycle plots for OBS-C-O and DBS-C models

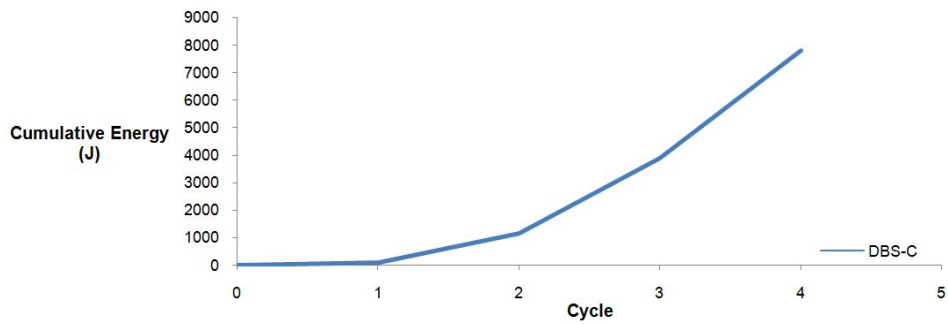


Fig. 21 Cumulative energy-loading cycle plot for DBS-C Model

Table 6 Analytical results obtained by force-energy and force-loading cycle plots

Models	Model OBS-C-O	Model DBS-C
$\Delta_{P-\max}$ (mm)	41.4	16.1
$\Delta_{E-\max}$ (mm)	5.06	4.6
$\sum_{i=1}^n E_i$ (J)	55016.67	7782
$\sum_{i=1}^m E_i$ (J)	96.08	100
$\frac{(\Delta_{P-\max} - \Delta_{E-\max})}{\Delta_{E-\max}}$	7.18	2.5
$\bar{E}_P = \frac{\left( \sum_{i=1}^n E_i - \sum_{i=1}^m E_i \right)}{(n - m)}$ (J)	9153.43	2560.67
$\bar{E}_E = \frac{\sum_{i=1}^m E_i}{m}$ (J)	96.08	100
$\frac{\bar{E}_P}{\bar{E}_E}$	95.27	25.61

In Fig. 17 energy-loading cycle plot and in Fig. 18 force-loading cycle plot of hinged frame with diagonal bracing system and ductile element are shown. The force - energy plot is also presented in Fig. 19. The high absorption of energy is increased by ductile element while the minimum variation of load is applied.

Figs. 20-21 respectively, have shown displacement-loading cycle plot and cumulative energy-loading cycle plot of hinged frame with Diagonal bracing system and ductile element. The obtained results of models are shown in Table 6.

As seen, the average energy per loading cycle in the nonlinear limit zone is 25.61 times more than the average energy per loading cycle linear limit zone and lateral nonlinear displacement of frame is 2.5 times more than the lateral linear displacement of it. Bearing capacity of the frame in nonlinear limit is 2.27 times more than the bearing capacity of it in linear limit. The average energy per loading cycle in nonlinear limit is 25.61 times more than average energy of it in linear limit.

### 7.2 Off-centre bracing system with ductile element in optimum place

The obtained results from the analysis of the model under cyclic load as a plot of force-displacement are presented in Fig. 22. This curve continued to ultimate yielding strain of applied steels. To investigate inelastic behavior, the Von Misses yield surface is utilized. In this analysis, tolerable tensile load in the nonlinear limit zone is 219.03 kN and tolerable compressive load in the nonlinear limit zone is 229.82 kN. The maximum displacement in the nonlinear zone of 41.4 mm is achieved.

The obtained hysteresis plot is very wide and revealed suitable absorption of input energy to the structure. As shown in Fig. 23, the hysteresis push force-displacement plot of frame is obtained. The maximum tolerable load in this system is 229.82 kN, the maximum displacement is 41.4 mm and the displacement of the system at the end of elastic limit is 5.06 mm. The ductility factor ( $\mu$ ) of this system is

$$\mu = \frac{\Delta_{\max}}{\Delta_y} = \frac{41.4}{5.06} = 8.18 \quad (16)$$

In Fig. 24 Von Misses stress distribution, Von Misses strain distribution of hinged frame with off-centre bracing system and ductile element are shown.

In Fig. 17 energy-loading cycle plot and in Fig. 18 force-loading cycle plot of hinged frame with off-centre bracing system and ductile element are shown.

The force - energy plot is shown in Fig. 19. As load increases, the gradient of curve is increased and in the last step of loading, curve gradient approximately reaches to gradient of vertical line. This applies the increase in extremely high energy absorption to the minimum variation of load.

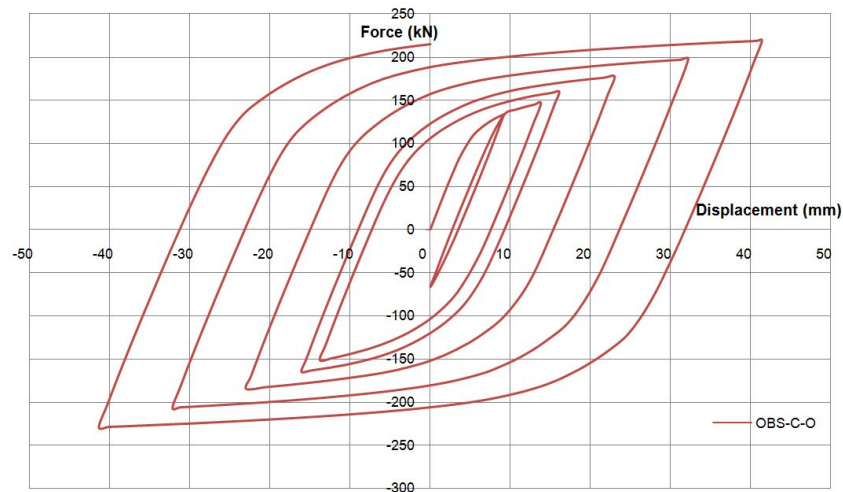


Fig. 22 Force-lateral displacement plot for OBS-C-O Model

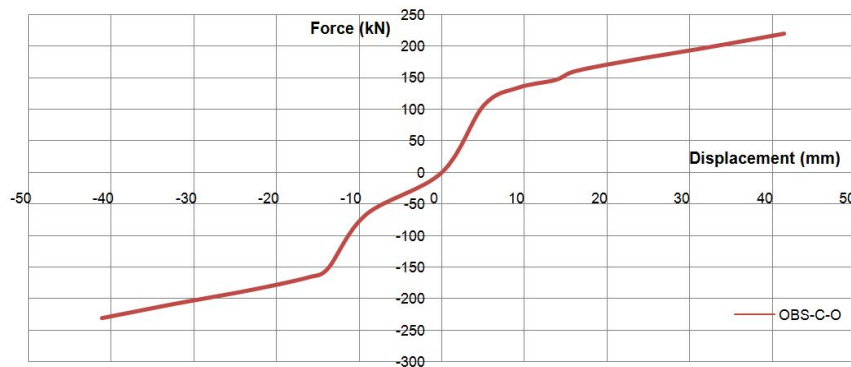


Fig. 23 Hysteresis loops push of force-displacement plot for OBS-C-O Model

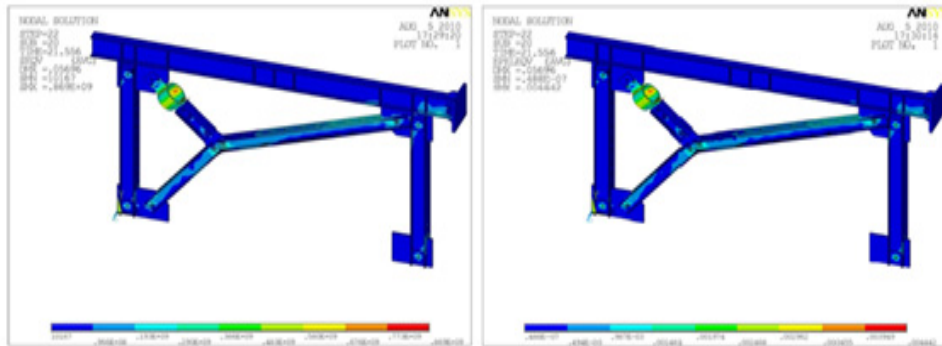


Fig. 24 Von Mises strain and stress under cyclic load for OBS-C-O Model

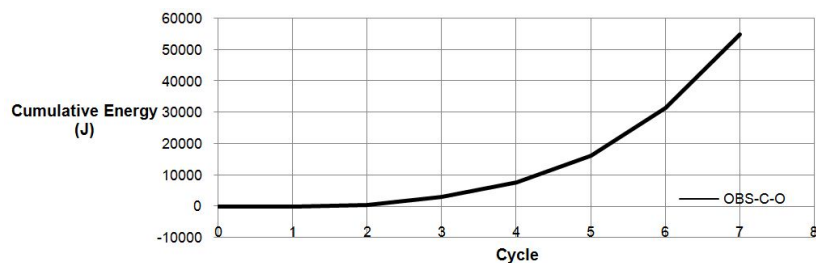


Fig. 25 Cumulative energy-loading cycle plot for OBS-C-O model

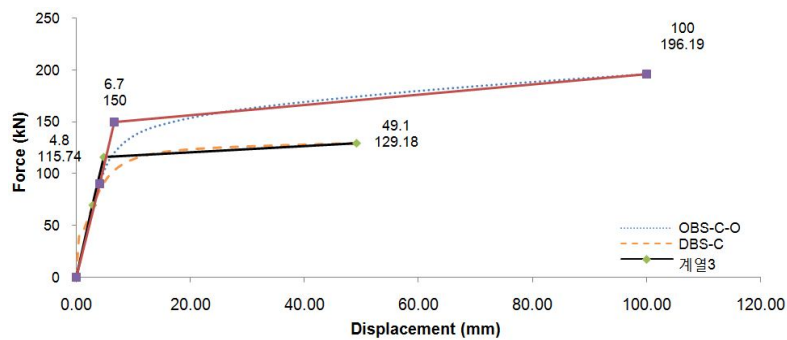


Fig. 26 Comparison between bilinear force-displacement curve of OBS-C-O and DBS-C models

Figs. 20 and 25 respectively, have shown displacement-loading cycle plot and cumulative energy-loading cycle plot of hinged frame with off-centre bracing frame and ductile element. As seen, the average energy per loading cycle in the nonlinear limit zone is 95.27 times more than the average energy per loading cycle linear limit zone and lateral nonlinear displacement of frame is 7.18 times more than the lateral linear displacement of it. Bearing capacity of the frame in nonlinear limit is 2.08 times more than bearing capacity of it in linear limit. The average energy per loading cycle in nonlinear limit is 95.27 times more than the average energy of it in linear limit. The obtained results revealed high energy dissipation in this system. The analytical results from these plots are shown in Tables 5 and 6.

## 8. Evaluating and comparing the finite element analysis results of models

### 8.1 Evaluating and comparison of monotonic load results

Fig. 26 have shown push over the curves of hinged frame with the off-centre bracing frame with the ductile element and the diagonal bracing system with the ductile element. The value of secondary hardness (38.8%), yielding force (22.84%), yielding force while displacement is 0.03H (34.16%), yielding displacement (28.36%), ductility factor (31.48%) and absorbed energy (65.66%) in OBS-C-O model were more than that of DBS-C model. However, the elastic stiffness in the DBS-C model was 6% more than that of OBS-C-O model. The above mentioned parameters are shown in Table 3.

### 8.2 Evaluating and comparison of cyclic load results

Plots of OBS-C-O and DBS-C models were compared for more accurate investigation of hysteresis curves. The most important specifications of them are represented in Figs. 17-20. As shown, the obtained results of the analysis are restricted to the ultimate strain of steels. In Fig. 27, the hysteresis curve of force-lateral displacement for model OBS-C-O, the maximum tolerable tensile load in the nonlinear limit zone of 219.03 kN, the maximum compressive load in the nonlinear limit zone for same model of 229.82 kN and also maximum displacement in this model in the nonlinear limit zone of 41.4 mm are obtained.

As shown in Fig. 17, the value of dissipated energy of the off-centre bracing system and the ductile element under cyclic load in model OBS-C-O of 23616.13 J is obtained, this value is approximately 6 times more than Model DBS-C with 3915.99 J. As shown in Fig. 18, the value of absorbing the force of the off-centre bracing system and the ductile element under cyclic load in model OBS-C-O of 222.81 kN is obtained, this value is approximately 2.09 times more than that of Model DBS-C with 104.84 kN. As shown in Fig. 19, comparison between plots of force-energy by the off-centre bracing system with the ductile element under cyclic load with diagonal ones revealed that the model OBS-C-O absorbed 222.81 kN force while dissipating 23616.13 J energy, these values are better than Model DBS-C with 104.84 kN and 3915.99 J. As shown in Fig. 27, lateral displacement of model OBS-C-O 41.4 mm is obtained, this value is approximately 2.57 times more than Model DBS-C with 16.1 mm.

## 9. Conclusions

The goal of this paper is increasing in ductility of off-centre brace by using ductile member and also highlighting the role of braces with circular element. Such braces have a suitable workability, ease of maintenance, as well as ductility and stability, preparing and installing with available material in the market and also replacing the system after damaging by hazardous earthquakes with low cost and high rate. Hence, it can make use of steel's properties while reducing the construction costs.

Investigating the hinged frame with the off-centre bracing frame with ductile element and the diagonal bracing system with the ductile element revealed that using a ductile element in order to increase the ductility of bracing systems is a valuable idea, increasing the ductility of eccentric bracing system lead to increase their application in the high-rise buildings. Hence, the ductility of bracing systems with the ductile element is considerably increased by using the same material. The

obtained results indicate that OBS-C-O model can be designed to behave like a base isolation system, with adequate reserved strength, to safeguard against instability in collapse level earthquakes. The performance of the steel ring at the end of braces system illustrating as a first defensive line and buckling fuse in the off-centre bracing system.

The research reveals that the idea of using a circular element as suggested in this paper supplying the mentioned goals. Furthermore, steel ring has been provided by industrial pipe and preparing of it in order to install in different braces would easily be created by contractors.

Considering all reasons like ductility, dissipated energy etc, analytical results of the off-centre bracing system with the ductile element and the diagonal bracing system with the ductile element showed that OBS-C-O model has more ductility and absorption of energy compared to DBS-C model. Ultimately, the steel ring welded to connections plates is a ductile element with high potential of dissipating energy that can be used in an off-centre brace frame where it would be more helpful than in diagonal brace frame.

## Acknowledgments

The first author would like to thank the Office of Gifted Students at Semnan University for financial support.

## References

- Abbasnia, R., Vetr, M.G.H., Ahmadi, R. and Kafi, M.A. (2008), "Experimental and analytical investigation on the steel ring ductility", *Sharif J. Sci. Technol.*, **52**, 41-48.
- Amadio, C., Clemente, I., Macorini, L. and Fragiocomo, M. (2008), "Seismic behaviour of hybrid systems made of PR composite frames coupled with dissipative bracings", *Earthq. Eng. Struct. Dyn.*, **37**(6), 861-879.
- American Institute of Steel Construction (AISC) (2005), Specification for structural steel buildings, Chicago, IL, USA.
- Andalib, Z., Kafi, M.A. and Bazzaz, M. (2010), "Using hyper elastic material for increasing ductility of bracing", *Proceedings of the 1st Conference of Steel & Structures and 2nd Conference on Application of High-Strength Steels in Structural Industry*, Tehran, Iran, December.
- Andalib, Z., Kafi, M.A., Kheyroddin, A. and Bazzaz, M. (2014), "Experimental investigation of the ductility and performance of steel rings constructed from plates", *J. Construct. Steel Res.*, **103**, 77-88.
- Annan, C.D., Youssef, M.A. and El Nagggar, M.H. (2009), "Experimental evaluation of the seismic performance of modular steel-braced frames", *J. Eng. Struct.*, **31**(7), 1435-1446.
- Applied Technology Council (ATC-24) (1996), Guidelines for cyclic seismic testing of components of steel structures; ATC, Redwood City, CA, USA.
- Bazzaz, M., Kheyroddin, A., Kafi, M.A. and Andalib, Z. (2011), "Evaluating the performance of steel ring in special bracing frame", *Proceedings of the 6th International Conference of Seismology and Earthquake Engineering*, Tehran, Iran, May.
- Bazzaz, M., Kheyroddin, A., Kafi, M.A. and Andalib, Z. (2012), "Evaluation of the seismic performance of off-centre bracing system with ductile element in steel frames", *Steel Compos. Struct., Int. J.*, **12**(5), 445-464.
- Bazzaz, M., Kheyroddin, A., Kafi, M.A., Andalib, Z. and Esmaeili, H. (2014), "Evaluating the seismic performance of off-centre bracing system with circular element in optimum place", *Int. J. Steel Struct.*, **14**(2), 293-304.
- Bazzaz, M., Andalib, Z., Kafi, M.A. and Kheyroddin, A. (2015), "Evaluating the performance of OBS-C-O

- in steel frames under monotonic load”, *Earthq. Struct., Int. J.*, **8**(3), 697-710.
- Federal Emergency Management Agency (FEMA) (2000), “Prestandard and commentary for the seismic rehabilitation of buildings”, Report No. FEMA 356; Washington, USA.
- Hsu, H.L., Juang, J.L. and Chou, C.H. (2011), “Experimental evaluation on the seismic performance of steel knee braced frame structures with energy dissipation mechanism”, *Steel Compos. Struct., Int. J.*, **11**(1), 77-91.
- Lotfollahi, M. and Mofid, M. (2008), “Innovative method in seismic design of slab-on-girder steel bridges”, *J. Construct. Steel Res.*, **64**(12), 1420-1435.
- Majidzamani, S., Vafaei, A., Aghakouchak, A.A. and Desai, C. (2011), “Experimental investigation of steel frames braced with symmetrical pairs of  $\gamma$ -shaped concentric bracings”, *J. Steel Struct.*, **11**(2), 117-131.
- Majidzamani, S. and Rasouli, M. (2006), “Experimental investigation of behavior of  $\gamma$ -shaped concentric steel bracing”, *Asian J. Civil Eng. (Building and Housing)*, **7**(1), 81-94.
- Marshall, J.D. and Charney, F.A. (2010a), “A hybrid passive control device for steel structures, I: Development and analysis”, *J. Construct. Steel Res.*, **66**(10), 1278-1286.
- Marshall, J.D. and Charney, F.A. (2010b), “A hybrid passive control device for steel structures, II: Physical testing”, *J. Construct. Steel Res.*, **66**(10), 1287-1294.
- Moghaddam, H. and Estekanchi, H. (1995), “On the characteristics of off-centre bracing system”, *J. Construct. Steel Res.*, **35**(3), 361-376.
- Moghaddam, H. and Estekanchi, H. (1999), “Seismic behavior of off-centre bracing systems”, *J. Construct. Steel Res.*, **51**(2), 177-196.
- Murthy, A.N.C.K. (2005), “Application of visco-hyperelastic devices in structural response control”, The degree of Master of Science; Civil Engineering Department, Blacksburg Polytechnic Institute, Virginia Polytechnic Institute and State University, Blacksburg, VA, USA.
- Roark, R.J. (1990), *Formulas for Stress and Strain*, McGraw-Hill Book Company.
- Singh, M.P. and Moreschi, L.M. (2002), “Optimal placement of dampers for passive response control”, *Earthquake Engineering and Structural Dynamics*, **31**(4), 955-976.
- Uang, C.-M. and Bertero, V.V. (1988), “Use of energy as a design criterion in earthquake-resistant design”, Technical Report UCB/EERC-88/18; University of California, Berkeley, CA, USA.
- Whittaker, A.S., Bertero, V.V., Thompson, C.L. and Alonso, L.J. (1991), “Seismic testing of steel plate energy dissipation devices”, *Earthquake Spectra*, **7**(4), 563-604.

### Abbreviation

$Q_y$	Yielding force
$\Delta_y$	Yielding displacement
$K_e$	Elastic stiffness
$K'$	Secondary hardness
$Q_{y\ 0.03}$	Yielding force while displacement is 0.03H
$E_{Monotonic}$	Absorbed energy under monotonic load
$\mu$	Ductility factor
$E_{P-max}$	Energy value in the last nonlinear cycle
$E_{E-max}$	Energy value in the last linear cycle
$P_{P-max}$	Force value in the last nonlinear cycle
$P_{E-max}$	Force value in the last linear cycle
$\frac{E_{P-max}}{E_{E-max}}$	The ratio of energy in the last nonlinear cycle of energy in the last linear cycle
$\frac{P_{P-max}}{P_{E-max}}$	The ratio of force in the last nonlinear cycle to force in the last linear cycle
$\Delta_{P-max}$	Lateral displacement of frame in the last nonlinear cycle
$\Delta_{E-max}$	Lateral displacement of frame in the last linear cycle
$\sum_{i=1}^m E_i$	Total energy in 6 loading cycles
$\sum_{i=1}^n E_i$	Total energy in 1 loading cycle
$\frac{(\Delta_{P-max} - \Delta_{E-max})}{\Delta_{E-max}}$	The ratio of nonlinear lateral displacement to Linear lateral displacement
$\bar{E}_E = \frac{\sum_{i=1}^n E_i}{n}$	Average energy per loading cycle in linear limit zone
$\frac{\bar{E}_P}{\bar{E}_E}$	The ratio of average nonlinear energy to average linear energy per loading cycle
$\delta_i$	Maximum displacement of loading
$n_i$	Number of cycles with $\delta_i$ displacement amplitude
$\Delta$	Yielding displacement of the damper